

# Quantum Dot Based on Z-shaped Graphene Nanoribbon: A First-principles Study

Hao Ren,<sup>1</sup> Qunxiang Li,<sup>1,\*</sup> Q. W. Shi,<sup>1</sup> and Jinlong Yang<sup>1,†</sup>

<sup>1</sup>*Hefei National Laboratory for Physical Sciences at Microscale,  
University of Science and Technology of China, Hefei, Anhui 230026, P.R. China*

(Dated: July 11, 2007)

## Abstract

The electronic and transport properties of the Z-shaped graphene nanoribbons heterojunction are investigated by a fully self-consistent non-equilibrium Green's function method combined with density functional theory. The first-principles calculations show that the robust quantum confinement effect in the junction can be used to design the quantum dot. The electronic states are confined by the topological structure of the junction. This kind of Z-shaped quantum dot can be realized regardless of doping impurity, edge chemical modification, and the length of junction. Moreover, the spatial distribution and the number of confined states are tunable.

**Key words:** quantum dot, Z-shaped graphene nanoribbons heterojunction, first-principles calculations

## I. INTRODUCTION

Carbon-based low-dimensional materials such as fullerenes and carbon nanotubes (CNTs) have attracted great attention since they are promising candidates of building blocks of future molecular devices.<sup>1,2</sup> Recently, a single layer of carbon sheet with hexagon honeycomb structures (named graphene) has been fabricated successfully.<sup>3,4</sup> Many experimental measurements of its structural and electronic properties have been performed.<sup>5,6</sup> Due to the linear energy dispersion relation near the Dirac points, this novel two dimensional material is an interesting conductor in which electrons move like massless Dirac-fermions with long elastic scattering lengths.<sup>6,7</sup>

Unlike CNTs, the flat structure of graphene can be tailored using conventional lithography techniques. Now it is possible to make graphene nanoribbons (GNRs) with width from several nanometers to micrometers.<sup>7,8</sup> There are two representative types of GNRs according to the edge configuration: armchair or zigzag. All GNRs with zigzag edge (ZGNRs) are metallic due to the two edge states degenerated at the Fermi level without considering the electron spin degree of freedom regardless of its width,<sup>9,10</sup> while the hydrogen-saturated armchair GNRs (AGNRs) are semiconductors and the energy gaps exhibit three distinct family behavior depending on its width.<sup>10,12</sup> In addition to the study of two-dimensional and one-dimensional electronic structures of graphene,<sup>11</sup> research attention has been focus on designing quantum dot.<sup>13,14</sup> Pereira *et al.* demonstrated theoretically that quantum dots can be designed in bilayer graphene through introducing a position-dependent doping.<sup>13</sup> Trauzettel *et al.* proposed that the confinement in AGNR quantum dot is achieved by tuning the voltages applied to the gates and proved that the spin qubits can not only be coupled between the nearest neighbor quantum dots but also over a long distances.<sup>14</sup> Recently, we discovered that a quantum dot can be realized in a Z-shaped GNRs junction basing on the nearest neighbor  $\pi$  orbital tight binding (TB) calculations.<sup>15</sup> The discrete confined states were observed regardless of substrate induced static disorder or edge irregularities in junction. However, the simple TB simulations fail to address the following issues: (1) Energy gaps of AGNRs are not predicted accurately using a single hopping parameter. For example, AGNRs with width of  $3p+2$  ( $p$  is an integer) are metallic at TB level, while the first-principles calculation shows that it is semiconductor.<sup>10,11</sup> (2) Geometric relaxation in the Z-shaped junction is not considered in the previous TB calculations. (3) Moreover, it

is also difficult to describe the impurity adsorbing, doping and edge chemical modification appropriately in TB model. Therefore it is desirable to perform first-principles calculations to reexamine our TB results.<sup>15</sup>

In this paper, the electronic and transport properties of such a Z-shaped GNRs heterojunction are investigated by a fully self-consistent non-equilibrium Green's function (NEGF) method combined with density functional theory (DFT). We find that the robust quantum confinement effect comes from its topological structure. Moreover, the theoretical results show that the spatial distribution and the number of confined states are tunable through doping, edge chemical modification and varying the length of junction.

## II. COMPUTATIONAL METHOD AND MODEL

The schematic view of our quantum dot made of Z-shaped junction is shown in Figure 1. This open system is constructed by two semi-infinite leads and a finite piece of central region. This kind of heterojunction is a typical two-probe system, which contains three parts: the left lead (L), the right lead (R) and the extended molecule region (EM). Here, the left and right leads are designed with AGNRs with width  $W=7$  to confine the electronic states in the central region. The EM part includes a piece of ZGNR and two surface layers of the left and right lead at both sides. The width and length of ZGNR is set to be 6 and 4 as shown in Fig. 1(b), respectively.

Our electronic structure calculations are carried out by using the first-principles self-consistent pseudopotential method implemented in SIESTA package.<sup>16</sup> The exchange-correlation effect and electron-ion interaction is described by the local density approximation and the norm-conserved pseudopotential in the fully nonlocal form,<sup>18-20</sup> respectively. A double- $\zeta$  plus polarization basis set is used to describe the localized atomic orbitals<sup>21</sup> and an energy cutoff for real space mesh size is set to be 380 Ry. All atomic positions of the leads and central region are fully relaxed with a force tolerance 0.01 eV/Å. For the semi-infinite leads, 32 K-points along the axial direction in the first Brillouin zone are used. The vacuum gaps between two neighboring planes and layers are set to be 22 Å.

The electron transport properties of this Z-shaped GNR junction are studied by using the real-space NEGF techniques implemented in TransSIESTA package.<sup>17,23</sup> The transmission spectrum is expressed as

$$T(E) = Tr[\Gamma_L(E)G(E)\Gamma_R(E)G^\dagger(E)], \quad (1)$$

where  $E$  stands for the injecting electron energy,  $\Gamma_{L(R)}$  and  $G(E)$  is the coupling matrix between the left (right) lead and the EM region, and the retarded Green's function, respectively, which are defined as

$$\Gamma_{L,R}(E) = i(\Sigma_{L,R}(E) - [\Sigma_{L,R}(E)]^\dagger), \quad (2)$$

$$G(E) = [ES - H_{eff}]^{-1}. \quad (3)$$

Here, the effective Hamiltonian of the EM region can be expressed as

$$H_{eff}(E) = H_{EM}(E) + \Sigma_L(E) + \Sigma_R(E) \quad (4)$$

where  $H_{EM}$  is the Hamiltonian of EM region, the contributions from the left (right) lead are included in the self-energy term  $\Sigma_{L(R)}$ . Once the converged effective Hamiltonian is achieved in the DFT-NEGF procedure under open boundary conditions in the two-probe system, we calculate the electronic structures of the extended region including the eigenvalues and corresponding eigenvectors. Here, these eigenvalues are referred as renormalized molecular levels (RMLs) since the effect of two electrodes is taken into account.<sup>22</sup>

To obtain the contribution to  $i$ th RML ( $\Psi_i^{RML}$ ) coming from the central ZGNR, we define the ratio ( $P_i$ ) as

$$P_i = \frac{\sum_{\mu \in ZGNR} D_{\mu i}}{\sum_{\mu \in EM} D_{\mu i}}, \quad (5)$$

where,  $D_{\mu i}$  is determined by<sup>16</sup>

$$D_{\mu i} = \sum_{\nu} C_{\mu i} \langle \phi_{\mu} | \phi_{\nu} \rangle C_{\nu i}, \quad (6)$$

here,  $C_{\mu i}$  is the combination coefficient of  $|\phi_{\mu}\rangle$  in  $\Psi_i^{RML}$ ,  $\phi_{\mu}$  is the non-orthogonal basis function. Actually, the denominator of Eq. (5) is equal to 1. In this part of calculations, the single- $\zeta$  basis set is used to describe the localized atomic orbitals and a mesh cutoff is set to be 150 Ry for saving computational time. Test calculations with the large basis set and cut off energy give similar results.

### III. RESULTS AND DISCUSSION

First, it is interesting to calculate the electronic structures of the semiconductor leads and the isolated central region (ZGNR). The band structure and density of states (DOS) of the optimized periodic leads are shown in Figure 2 (a). The relaxed inner and edge C-C distance is about 1.42 and 1.37 Å, and the direct energy gap at  $\Gamma$  point of the AGNR with width  $W=7$  is about 1.62 eV (from -0.81 to 0.81 eV), which agree well with the pervious DFT results.<sup>10,11</sup> For the isolated ZGNR, its DOS is calculated by a Lorentzian extension of the discrete states, and the broadening width is set to be 0.025 eV. Clearly, there are two discrete states at  $\pm 0.33$  eV as shown in Fig. 2 (b), which locate within the energy gap of the semiconducting leads and correspond to the highest occupied molecular orbital (HOMO) and the lowest unoccupied molecular orbital (LUMO). In principle, this observation implies that it is possible to use the potential well contributed by two semiconducting leads to confine two states of the central region.

Due to the presence of two semiconducting leads, the electronic and transport properties of the model Z-shaped heterojunction are obtained fully self-consistent by using DFT-NEGF technique.<sup>23</sup> Figure 3 (a) presents the calculated transmission spectrum. Clearly, no appreciable transmission appears in the wide bias window (i.e. from -0.75 to 0.75 eV, here, we name it as the transmission gap). It means that these electrons locating within this energy range can not transport through the Z-shaped junction. The transmission gap originates from the energy band gap of two AGNRs leads. Interesting, we find that there are four RML confined discrete states, which locates at -0.47, -0.36, -0.26, and 0.24 eV relative to the Fermi level labeling with A, B, C, and D in Fig. 3 (a), respectively. This observation demonstrates clearly that these discrete states are caused by quantum confinement, which produces the main feature of our previous TB observation.<sup>15</sup> This kind of Z-shaped heterojunction can, therefore, be used as a quantum dot device. Actually, the similar quantum confinement is observed in quantum dots based on CNT through introducing pentagon-heptagon defects, for example, a (6,4)/(5,5)/(6,4) CNT system.<sup>24</sup> It should be pointed out that in previous designs basing on GNRs, the quantum confinement is achieved by doping or applying the gate voltage,<sup>13,14</sup> here, in our model device the confinement originates from the topological structure of the junction. That is to say, the discrete states are confined within the surrounding potential barriers contributed by the energy gaps of two AGNR leads with finite

width.

However, the DFT results are not consistent quantitatively with our previous TB results.<sup>15</sup> In TB calculations, the C-C distance is fixed to be 1.42 Å in Z-shaped junction and the electronic properties are simulated by a single hopping parameter ( $\gamma=-2.66$  eV). It means that the Z-shaped GRNs junction has electron-hole symmetry. The energy gap of AGNR with width  $W=7$  is underestimated to be about 1.22 eV at TB level. Only two sharp peaks locate symmetrically around the Fermi level ( $\pm 0.3$  eV). While the atomic positions are allowed to relax in our DFT calculations, the C-C distances at interfaces vary about 3.0 % as shown in Fig. 1 (b). This kind of relaxed geometric structure breaks down the electron-hole symmetry, which leads to the RMLs locating around Fermi level asymmetrically. To examine the spatial distribution of these confined RMLs, we calculate the contribution to the four RMLs coming from ZGNR. The calculated results with Eq. (4) are shown in the right panel of Fig. 3(a). It is clear that the ZGNR region contributes about 56.8 and 70.7 % to two discrete states (A and D) at -0.47 and 0.24 eV, respectively. This result indicates that two discrete states are confined mainly at the central ZGNR region. Other two discrete states (B and C) at -0.36 and -0.26 eV have considerable component coming from the surface layers of AGNRs. As an example, the spatial distributions of one confined state labeled with *D* within the transmission gap is presented in Fig. 3 (b). Clearly, this state localizes at the central ZGNR region.

Now we turn to investigate the impact coming from the length of central ZGNR on quantum confinement in this kind of Z-shaped junction. Here, as an example, we extend the ZGNR length from  $L=4$  to 8. The transmission curve and the RMLs within the transmission gap are shown in Figure 4. As expected, the number of states locating within the transmission gap increases when the length of junction is extended, and the interval between these discrete confine states reduces. As shown in Fig. 4, six discrete states (RMLs) locate within the transmission gap at -0.48, -0.34, -0.27, -0.05, 0.06 and 0.43 eV, which is labeled with A, B, C, D, E, and F, respectively. From the right panel of Fig. 4, it is clear that among them four of these discrete states (A, D, E, and F) localize mainly at the ZGNR region. In our previous TB simulation, four confined states were observed for the same Z-shaped junction.<sup>15</sup> Clearly, another feature should be pointed out is that the ZGNR region contributes differently comparing with the right panel of Fig. 3 (a). These observations indicate that the spatial distribution and number of confined states are tunable through

varying the length of junction. This offers opportunity to control the electronic properties of the quantum dot based on this kind of Z-shaped GNR junction.

N- or B-doped CNT have been synthesized and investigated intensively in the recent years since doping is an attractive way to tailor the electronic and transport properties of CNTs.<sup>25</sup> Very recently, the field effect transistors and spin filters were predicted theoretically based on these N- and B-doped GNRs.<sup>26,27</sup> In fact, the perfect GNRs seldom exists in reality. So it is interesting to examine the quantum confinement in the doped quantum dot. Here, one carbon atom at site “D” in Fig. 1 (b) is substituted with one N or B atom, respectively. In the N doping junction, the geometric distortion is neglectable. The relaxed N-C distance is 1.39 Å, which is slightly less than the C-C bondlength (1.42 Å). The transmission spectrum and the RMLs locating in the transmission gap are shown in Figure 5 (a). Theoretical results indicate that within the transmission gap five discrete states locate at -0.63, -0.41, -0.35, 0.0, and 0.54 eV, labeled with A, B, C, D, and E, respectively. As seen in right panel of Fig. 5 (a). three of these states (A, D, and E) are mainly contributed by the central ZGNR. Comparing with the undoped Z-shaped junction, the positions of RMLs shift obviously after N substitution. Note that, one RML confined mainly at ZGNR region, D state, is the singly occupied molecular orbital (SOMO), which locates exactly at the Fermi level. For the B-doped junction, despite the different electron occupation of B atom, it is clear that once again the doping can not change the quantum confinement obviously. Five discrete confined states locate at -0.56, -0.37, -0.22, 0.0, and 0.52 eV as shown in Fig. 5 (b). Three of RMLs (A, D, and E) localize mainly at the central ZGNR region and D state is the SOMO locating at the Fermi level. Obviously, in the doped Z-shaped junctions, we observe the quantum confinement effect. There are several discrete states are confined mainly in the central ZGNR region, but their positions are tuned slightly through doping.

Due to the unique chemical reactivity of ZGNRs, the edged carbon atom could be passivated by various atoms or functional groups.<sup>28</sup> The edge modification on the quantum confinement is examined through substituting two hydrogen atoms at site “H1” and “H2” in the zigzag region with two F atoms as shown in Fig. 1 (b). Figure 6 (a) shows the calculated transmission spectrum and RMLs. Clearly, there is not significant change compared with Fig. 3 (a). Four states locate at -0.43, -0.36, -0.21, and 0.29, respectively. Comparing with the H-passivated junction, we find that the spatial distribution of these RMLs of three discrete confined states displays very similar feature, except somewhat distribution appears

at F sites in the F-passivated system. From the calculated projected density of states of fluorine atoms and their neighboring carbon atoms, as shown in Fig. 6 (b), one can see that near the Fermi level there are small peaks contributed by the  $p_z$  orbitals of F atoms, which takes part in the delocalized  $\pi$  states, while the other orbitals locate far away from the Fermi energy. The edge modification with F atom just changes the electronic structures of junction slightly and do not affect the robustness of the quantum confinement of the Z-shaped GNR heterojunction.

#### IV. CONCLUSION

In summary, the electronic structures and transport properties of Z-shaped heterojunctions (AGNR-ZGNR-AGNR) are studied by using a fully self-consistent NEGF combined with DFT. Present DFT results agree qualitatively with our previous TB simulations. The quantum confinement is achieved by introducing the topological structure in this kind of Z-shaped junction. The observed robust quantum confinement is not broken by doping, edge chemical modification, and varying the length of the ZGNR, while the spatial confinement and the number of discrete states are modified. These theoretical findings provide a possible way to fabricate quantum dot based on this kind of Z-shaped structure.

#### ACKNOWLEDGMENT

This work was partially supported by the National Natural Science Foundation of China under Grant Nos. 10674121, 10574119, 50121202, and 20533030, by National Key Basic Research Program under Grant No. 2006CB922000, by the USTC-HP HPC project, and by the SCCAS and Shanghai Supercomputer Center.

---

\* Corresponding author. E-mail: liqun@ustc.edu.cn

† Corresponding author. E-mail: jlyang@ustc.edu.cn

<sup>1</sup> H. W. Kroto, J. R. Heath, S. C. O'Brien, R. F. Curl and R. E. Smalley, *Nature* **318**, 162 (1985).

<sup>2</sup> S. Iijima and T. Ichibashi, *Nature* **363**, 603 (1993).



- <sup>3</sup> K. S. Novoselov, A. K. Geim, S. V. Morozov, D. Jiang, Y. Zhang, S. V. Dubonos and A. A. Frisov, *Nature* **438**, 197 (2005).
- <sup>4</sup> Y. B. Zhang, Y. W. Tan, H. L. Stormer and P. Kim, *Nature* **438**, 201 (2005).
- <sup>5</sup> J. S. Bunch, A. M. van der Zande, S. S. Verbridge, I. W. Frank, D. M. Tanenbaum, J. M. Parpia, H. G. Craighead and P. L. McEuen, *Science* **315** 490(2007).
- <sup>6</sup> C. Berger, Z. Song, X. Li, X. Wu, N. Brown, C. Naud, D. Mayou, T. Li, J. Hass, A. N. Marchenkov, E. H. Conrad, P. N. First and W. A. de Herr, *Science* **312**, 1191 (2006).
- <sup>7</sup> A. K. Geim and K. S. Novoselov, *Nature Mater.* **6**, 183 (2007).
- <sup>8</sup> M. Y. Han, B. Özyilmaz, Y. B. Zhang and P. Kim, *Phys. Rev. Lett.* **98**, 206805 (2007).
- <sup>9</sup> M. Fujita, K. Wakabayashi, K. Nakada and K. Kusakabe, *J. Phys. Soc. Jpn.* **65**, 1950 (1996).
- <sup>10</sup> Y.-W. Son, M. L. Cohen and S. G. Louie, *Phys. Rev. Lett.* **97**, 216803 (2006); Y.-W. Son, M. L. Cohen and S. G. Louie, *Nature* **444**, 347 (2006).
- <sup>11</sup> Z. F. Wang, Qunxiang Li, Haibin Su, Xiaoping Wang, Q. W. Shi, Jie Chen, Jinlong Yang, and J. G. Hou, *Phys. Rev. B* **75**, 085424 (2007); Z. F. Wang, Qunxiang Li, Huaixiu Zheng, Hao Ren, Haibin Su, Q. W. Shi and Jie Chen, *Phys. Rev. B* **75**, 113406 (2007).
- <sup>12</sup> V. Barone, O. Hod and G. E. Scuseria, *Nano Lett.* **6**, 2748 (2006).
- <sup>13</sup> J. M. Pereira, Jr., P. Vasilopoulos and F. M. Peeters, *Nano Lett.* **7**, 946 (2007).
- <sup>14</sup> B. Trauzettel, D. V. Bulaev, D. Loss and G. Burkard, *Nature Phys.* **3**, 192 (2007).
- <sup>15</sup> Z. F. Wang, Huaixiu Zheng, Yao Yao, Q. W. Shi, Jie Chen, Qunxiang Li, Xiaoping Wang and J. G. Hou, *Appl. Phys. Lett.* (accepted, to be published).
- <sup>16</sup> J. M. Soler, E. Artacho, J. D. Gale, A. García, J. Junquera, P. Ordejón and D. Sánchez-Portal, *J. Phys.: Condens. Matter* **14**, 2745 (2002).
- <sup>17</sup> S. Datta, *Electronic Transport in Mesoscopic Systems*, Cambridge: Cambridge University Press, (1995)
- <sup>18</sup> J. P. Perdew and Alex Zunger, *Phys. Rev. B* **23**, 5048 (1981).
- <sup>19</sup> D. R. Hamann, M. Schlüter and C. Chiang, *Phys. Rev. Lett.* **43**, 1494 (1979).
- <sup>20</sup> L. Kleinman and D. M. Bylander, *Phys. Rev. Lett.* **48**, 1425 (1982).
- <sup>21</sup> J. Junquera, Ó. Paz, D. Sánchez-Portal and E. Artacho, *Phys. Rev. B* **64**, 235111 (2001).
- <sup>22</sup> B. Larade, J. Taylor, Q. R. Zheng, H. Mehrez, P. Pomorski and H. Guo, *Phys. Rev. B* **64**, 195402 (2001).
- <sup>23</sup> M. Brandbyge, J. L. Mozos, P. Ordejón, J. Taylor and K. Stokbro, *Phys. Rev. B* **65**, 165401

- (2002); J. Taylor, H. Guo and J. Wang, Phys. Rev. B **63**, 245407 (2001).
- <sup>24</sup> L. Chico, M. P. López Sancho and M. C. Muñoz, Phys. Rev. Lett. **81**, 1278 (1998).
- <sup>25</sup> M. Terrone, A. J. M. Endo, A. M. Rao, Y. A. Kim, T. Hayashi, H. Terrones, J.-C. Charlier, G. Dresselhaus and M. S. Dresselhaus, Mater. Today **7**, 30 (2004).
- <sup>26</sup> Q. M. Yan, B. Huang, J. Yu, F. W. Zheng, J. Zhang, J. Wu, B. L. Gu, F. Liu and W. H. Duan, Nano Lett. **7**, 1469 (2007).
- <sup>27</sup> T. B. Martins, R. H. Miwa, A. J. R. da Silva and A. Fazzio, Phys. Rev. Lett **98**, 196803 (2007).
- <sup>28</sup> D. E. Jiang, B. G. Sumpter and S. Dai, J. Chem. Phys **126**, 134701 (2007).

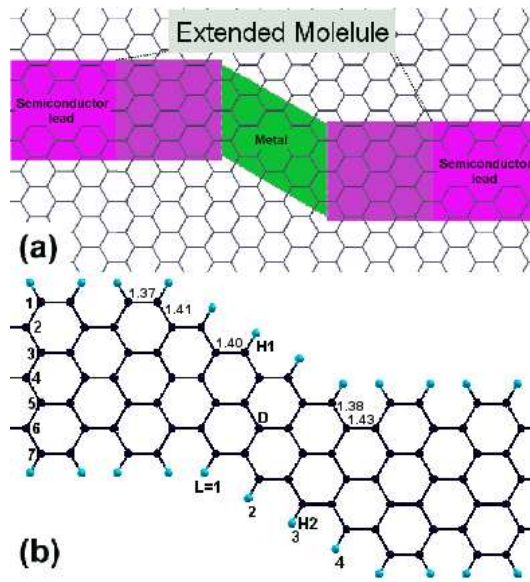


FIG. 1: (Color online) (a) A schematic of a quantum dot made of a Z-shaped GNR junction. (b) Atomic structure of the scattering region. Here, the electrodes are modeled by AGNRs with width  $W=7$ , the length and width of the central ZGNR is set to be 4 and 8, respectively.

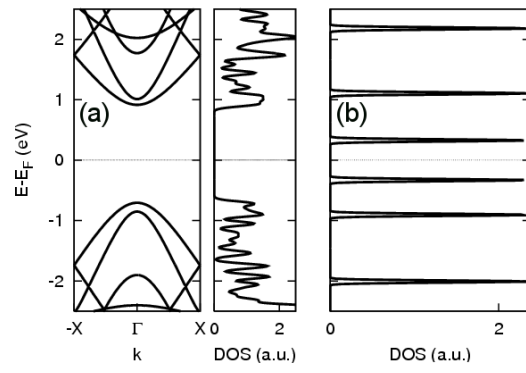


FIG. 2: (a) Band structure and DOS of the semiconducting lead. (b) DOS of the isolated central region (ZGNR).

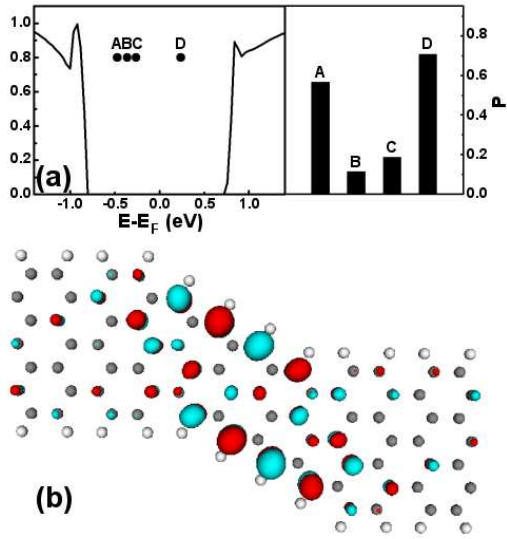


FIG. 3: (Color online) Transmission spectrum of H-passivated junction with the central zigzag region with length  $L=4$ . Filled circles stand for the positions of the RMLs. Right panel represents the contribution coming from the central ZGNR region. (b) The isosurface of the spatial distribution of one confined state (labeled with D), here the red and blue color stands for the positive and negative value of the corresponding wave function, respectively.

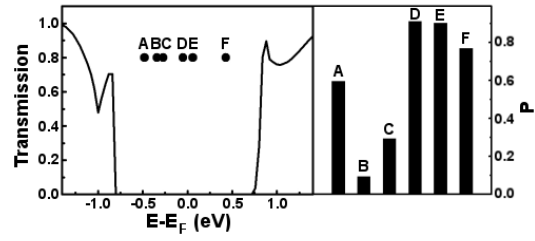


FIG. 4: Transmission spectrum of H-passivated junction with the central ZGNR with length  $L=8$ . Filled circles represent the positions of the RMLs. Right panel represents the contribution coming from the central ZGNR region.

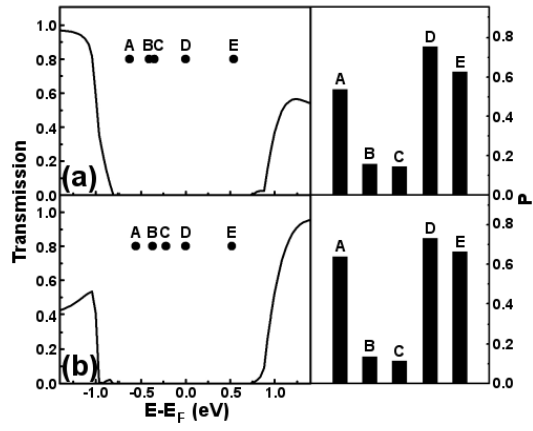


FIG. 5: Transmission spectrum of N-doped (a) and B-doped (b) Z-shaped junctions. Filled circles stand for the positions of RMLs. Right panels indicate the contribution coming from the ZGNR.

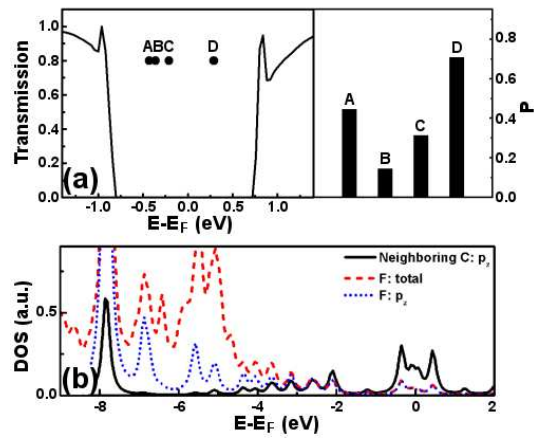


FIG. 6: (Color online) (a) Transmission spectrum of the F-modified Z-shaped junction. Filled circles stand for the positions of RMLs. Right panel shows the contribution from the ZGNR. (b) The projected density of states (PDOS) of F and neighboring C atoms in the F passivated junction.